Assessing cellular toxicities in fibroblasts upon exposure to lipid-based nanoparticles: a high content analysis approach



2011 Nanotechnology 22 494016

(http://iopscience.iop.org/0957-4484/22/49/494016)

Nanotechnology **22** (2011) 494016 (6pp) doi:10.1088/0957-4484/22/49/494016

# Assessing cellular toxicities in fibroblasts upon exposure to lipid-based nanoparticles: a high content analysis approach

**Leonardo J Solmesky[1,2,4], Michal Shuman[2,3,4], Meir Goldsmith[2,3], Miguel Weil[1,2] and Dan Peer[2,3]**

[1] Cell Screening Facility for Personalized Medicine, Laboratory for Neurodegenerative Diseases and Personalized Medicine, Tel Aviv University, Tel Aviv 69978, Israel
[2] Department of Cell Research and Immunology, George S Wise Faculty of Life Sciences, Tel Aviv University, Tel Aviv, 69978, Israel
[3] Laboratory of Nanomedicine, Center for Nanoscience and Nanotechnology, Tel Aviv University, Tel Aviv 69978, Israel

E-mail: miguelw@tauex.tau.ac.il and peer@post.tau.ac.il

Received 7 June 2011, in final form 5 August 2011
Published 21 November 2011
Online at stacks.iop.org/Nano/22/494016

**Abstract**
Lipid-based nanoparticles (LNPs) are widely used for the delivery of drugs and nucleic acids. Although most of them are considered safe, there is confusing evidence in the literature regarding their potential cellular toxicities. Moreover, little is known about the recovery process cells undergo after a cytotoxic insult. We have previously studied the systemic effects of common LNPs with different surface charge (cationic, anionic, neutral) and revealed that positively charged LNPs ((+)LNPs) activate pro-inflammatory cytokines and induce interferon response by acting as an agonist of Toll-like receptor 4 on immune cells. In this study, we focused on the response of human fibroblasts exposed to LNPs and their cellular recovery process. To this end, we used image-based high content analysis (HCA). Using this strategy, we were able to show simultaneously, in several intracellular parameters, that fibroblasts can recover from the cytotoxic effects of (+)LNPs. The use of HCA opens new avenues in understanding cellular response and nanotoxicity and may become a valuable tool for screening safe materials for drug delivery and tissue engineering.

## 1. Introduction

Lipid-based nanoparticles (LNPs) are widely used for therapeutic delivery of small molecules, peptides and nucleic acids [1–3]. The nature, shape and charge of the biomaterials, which are the raw materials constructing these LNPs, affect the interaction with different cell types. Several studies have laid the foundations for investigating the immune response when developing novel biomaterials and they focused mainly on lymphocytes and complement activation [4, 5] or examined global cell counts of leukocyte subsets when injecting novel formulations into animal models [6, 7].

We have recently studied the effect of LNPs on immune cells *in vivo* and revealed that only positively charged (+)LNPs induced a robust pro-inflammatory cytokine and interferon response by acting as an agonist with Toll-like receptor 4 (TLR4) expressed on monocytes and macrophages [8].

In the present study, we investigated the cytotoxicity response to LNPs in human fibroblasts as a cellular model system. Moreover, we determined the potential cellular toxicities and observed cell recovery upon exposure to LNPs. We utilized an image-based high content analysis (HCA)

[4] LJS and MS contributed equally to this work.

 

approach to determine sub-cellular changes upon exposure to LNPs reflected at the single pixel level.

Image-based HCA is a technology for high throughput microscopic analysis of cells that allows one to study cell behavior in depth. It involves probing cells with fluorescent markers, capturing images of the cells very rapidly with high-resolution image instrumentation and extracting detailed information from the images with powerful high content imaging software [9]. This software is able to segment each different compartment (according to pixel level of intensity) within a cell that has been traced by a given fluorescent marker, allowing the quantification of numerous parameters for each of the segmented compartments and the relation between these sub-cellular compartments [10]. Thus, the effect of a given molecule or drug carrier on the intrinsic cell biology can be intensively investigated. Based on these abilities of HCA, we have chosen this approach for studying the recovery of fibroblasts from toxicity induced by treatment with LNPs.

## 2. Materials and methods

### *2.1. Materials*

High-purity hydrogenated soy phosphatidylcholine (HSPC) and 1,2-distearoylphosphatidylglycerol (DSPG) were a kind gift from Lipoid GmbH (Ludwigshafen, Germany). 1,2-Dioleoyl-3-trimethylammonium-propane (DOTAP) was purchased from Avanti Polar Lipids Inc. (Alabaster, AL, USA). Cell culture plates and dishes were from Corning (New York, NY, USA). Human fibroblasts were cultured in Dulbecco's modified Eagle's medium (DMEM) (Gibco) supplemented with 1% pyruvate (Gibco), 1% penicillin/streptomycin/nystatin (Biological Industries, Israel) and 10% FCS (Hyclone). Polycarbonate membranes were from Nucleopore (Pleasanton, CA, USA). The following cellular fluorescent markers were used: Hoechst 33342 from Sigma-Aldrich (St Louis, MI, USA), calcein AM and Mitotracker from Invitrogen Life Technologies (Carlsbad, CA, USA). All other reagents were of analytical grade.

### *2.2. Preparation of lipid-based nanoparticles*

Lipid-based nanoparticles were prepared as previously described [8]. Three types of LNP were prepared: charge neutral LNPs composed of HSPC; negatively charged [8] composed of HSPC:DSPG at a 2:3 molar ratio; and positively charged [8] composed of HSPC:DOTAP at a 2:3 molar ratio. Briefly, multilamellar vesicles (MLV) were prepared by a lipid-film method and evaporated to dryness using a Buchi rotary evaporator [4, 8, 11]. The lipid film was hydrated with phosphate-buffered saline pH 7.4 to create MLV. Lipid mass was measured as previously described [4]. The resulting MLV were extruded into small unilamellar nano-scale vesicles with a Thermobarrel Lipex extruder™ (Lipex Biomembranes Inc., Vancouver, BC, Canada) at 60 °C under nitrogen pressures of 300–550 psi. The extrusion was carried out in a stepwise manner using membranes with progressively decreasing pore size (from 1, 0.8, 0.6, 0.4, 0.2, to 0.1 $\mu$m) (Nucleopore, Whatman), with 10 cycles per pore size. LNPs, (−)LNPs and (+)LNPs were stored at 4 °C until further use and for no more than 4 weeks.

### *2.3. Particle size distribution and zeta potential measurements*

The particle size distribution and mean diameter of LNPs, (−)LNPs or (+)LNPs were measured on a Malvern Zetasizer Nano ZS zeta potential and dynamic light scattering instrument (Malvern Instruments, Southborough, MA) using the automatic algorithm mode and analyzed with the PCS 1.32a as previously reported [4, 8, 11]. All measurements were done in 0.01 mol $l^{-1}$ NaCl, pH 6.7 at room temperature.

### *2.4. Cell viability assay*

Human fibroblasts were seeded onto 96-well plates ($1 \times 10^4$ cells/well). Twenty-four hours later, the medium was replaced by treatment medium that contained 10–100 $\mu$g $ml^{-1}$ LNPs. Either 3 or 8 h later, the treatment medium was removed, the cells were washed with PBS and the values of cell viability/well were determined by a colorimetric XTT assay [12] for the quantification of cell proliferation and viability (Biological Industries, Beit-Haemek, Israel). On the day of measurement, 0.1 ml of activation solution was added to 5 ml of XTT reagent to produce the reaction solution. Fifty microliters of this reaction solution was added to each well and incubated for 2–5 h according to the manufacturer's instructions. Then, the absorbance of each sample (450 nm) was measured against a background control (630 nm) using a Multiskan EX microplate photometer (Thermo Scientific, Hudson, NH, USA). Cells cultured in medium without LNPs served as a control.

### *2.5. Image-based high content analysis: acquisition and analysis*

Human primary fibroblasts incubated in medium supplemented with 100 $\mu$g $ml^{-1}$ (+)LNPs for 8 h at 37 °C were washed with fresh (LNP-free) medium and were either imaged immediately or subjected to recovery for two additional days in LNP-free medium. Cells cultured in medium without LNPs served as a control. At each mentioned time point (immediately after LNP removal and after 2 days' recovery), both (+)LNP treated cells and control cells were stained with Hoechst 33342 (Sigma-Aldrich), calcein AM and Mitotracker (Invitrogen) for 30 min at 37 °C and subjected to image acquisition using the In Cell Analyzer 2000 (GE Healthcare, UK). The image stacks produced were used to analyze several nuclear, cytoplasmic and mitochondrial parameters among the whole population using the In Cell Investigator 1.6 software (GE Healthcare, UK).

### *2.6. Statistical analysis*

Data were analyzed using two-way ANOVA with significance between treatment groups determined by Bonferroni post-tests.

## 3. Results and discussion

### *3.1. Particle size distribution and surface charge measurements*

To investigate whether surface charged LNPs induce toxic effects in fibroblasts, we prepared three types of LNP differing

**Table 1.** Hydrodynamic diameter and zeta potential measurements of neutral, positively and negatively charged LNPs. Each result is an average (±standard deviation) of six independent measurements. Particles were measured at pH 6.7, in double-distilled (dd) $H_2O$ with 10 mM NaCl, at 20 °C using a Malvern ZS Zetasizer.

| LNP type | NP lipid composition (molar ratio) | Hydrodynamic diameter (nm) | $z$ potential (mV) |
|---|---|---|---|
| LNPs | HSPC (1) | $98 \pm 13$ | $-5.8 \pm 1.3$ |
| (−)LNPs | HSPC:DSPG (2:3) | $101 \pm 10$ | $-53.7 \pm 5.3$ |
| (+)LNPs | HSPC:DOTAP (2:3) | $108 \pm 16$ | $+60.3 \pm 5.5$ |

in their surface charge, namely anionic, cationic and neutral in charge LNPs. All LNPs were composed of HSPC, which formed the basic lipid nanoparticle structure, while positively charged nanoparticles and negatively charged LNPs were composed with the addition of DOTAP or DSPG, respectively. The quaternary ammonium head group in the DOTAP lipid contributed a positive charge to the nanoparticles, while the addition of DSPG with its orthophosphate moiety donated a negative charge to the nanoparticles. Dynamic light scattering and surface charge (zeta potential) measurements were used to characterize and validate the hydrodynamic diameter of the LNPs and the charge of all three types of LNP. As shown in table 1, the average LNP size was in the range of 100 nm diameter for all formulations with a narrow size distribution, as evidenced by the small values of standard deviation. LNPs composed of HSPC alone had a zeta potential of –5.8 mV, confirming their neutral charge at the measured pH. An addition of 60% in the molar ratio of DSPG in the formulation changed the charge of the particles to negative (∼−53.7 mV), while increasing 60% in the molar ratio of DOTAP made the particles positively charged (∼+60 mV).

### *3.2. LNP induced cellular toxicity in fibroblasts*

All three types of LNP (cationic, anionic and neutral) were incubated at various concentrations (10, 30 and 100 $\mu$g ml$^{-1}$) either for 3 or 8 h on fibroblasts, as detailed in the materials and methods section. Cell viability was determined by the XTT assay in comparison to control (untreated) cells. A short incubation time of 3 h was sufficient (only at the highest concentration of (+)LNPs) to start inducing cell death. Anionic and neutral charge LNPs did not affect the fibroblasts' viability (figure 1(A)). Upon 8 h exposure, even at the lowest concentration, (+)LNPs showed signs of toxicity (figure 1(B)) in a dose dependent manner, whereas no toxicity was found for (−) LNPs or LNPs. Cationic nanoparticles have been studied in various cell types and found to induce mitochondrially mediated apoptosis in primary leukocytes, epithelial cells and in various cell lines [8, 13–16]. A study into the cytotoxicity of polyamine-based nanoparticles [17], which employed three clinically relevant cell lines (lymphoid, endothelial, and hepatic) to determine the cellular effects, found that all cells studied generated a significant release of lactate dehydrogenase (LDH) within the first hour of exposure to the cationic nanoparticles that was continued in a time dependent manner. Concomitantly rapid redistribution (30 min) of phosphatidylserine (PS) from the inner plasma membrane of the mitochondrion to the outer cell surface was observed.

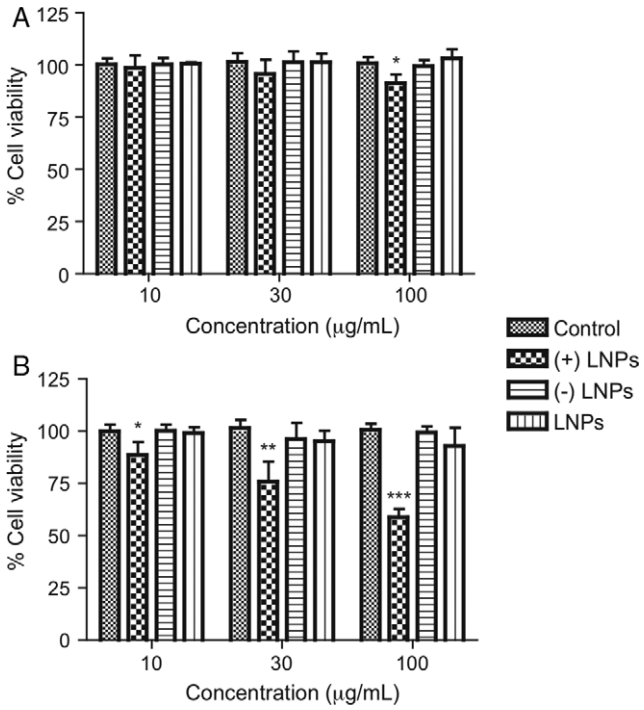


**Figure 1.** (+)LNPs induce cell death in a concentration dependent manner when incubated with fibroblasts for 3 or 8 h. (A) Cell viability (assayed by XTT cell viability assay) normalized to control (untreated cells) 3 h post-exposure to different types of LNP (+, −, and neutral; see Materials and Methods for composition) in various concentrations (10, 30 and 100 $\mu$g ml$^{-1}$). (B) Cell viability with the same conditions as listed above, normalized to control after 8 h of exposure. *, ** and *** denote $p < 0.05$, $p < 0.01$ and $p < 0.001$, respectively.

### *3.3. Fibroblast recovery upon exposure to LNPs*

Upon determining the cytotoxicity attributed to (+)LNPs, we investigated, by means of image-based HCA, whether the cells that survived the cytotoxic effect could in fact recover from this insult. To this end, we subjected fibroblasts either to the highest concentration tested (100 $\mu$g ml$^{-1}$) of (+)LNPs in culture medium or to medium without LNPs. Eight hours post-exposure cells were washed to eliminate excess of (+)LNPs and were either immediately stained for HCA with Hoechst 33342 (for staining the nucleus), calcein AM (for visualizing the cytoplasm and determining cell viability) and Mitotracker (for staining the live mitochondria) or allowed to recover for two additional days in culture medium before staining and image acquisition. Following the staining, images were acquired in the In Cell analyzer 2000 and analyzed using In Cell Investigator 1.6 software (both GE Healthcare). The software and the high-resolution images allowed quantification of numerous parameters at the cellular level. Representative images of the stained cells are presented in figure 2. It becomes apparent, in comparison to untreated cells (figures 2(A)–(D)), that 8 h of treatment with (+) LNPs (figures 2(E)–(H)) inflicts a decrease in cell density and in cell viability (as indicated by

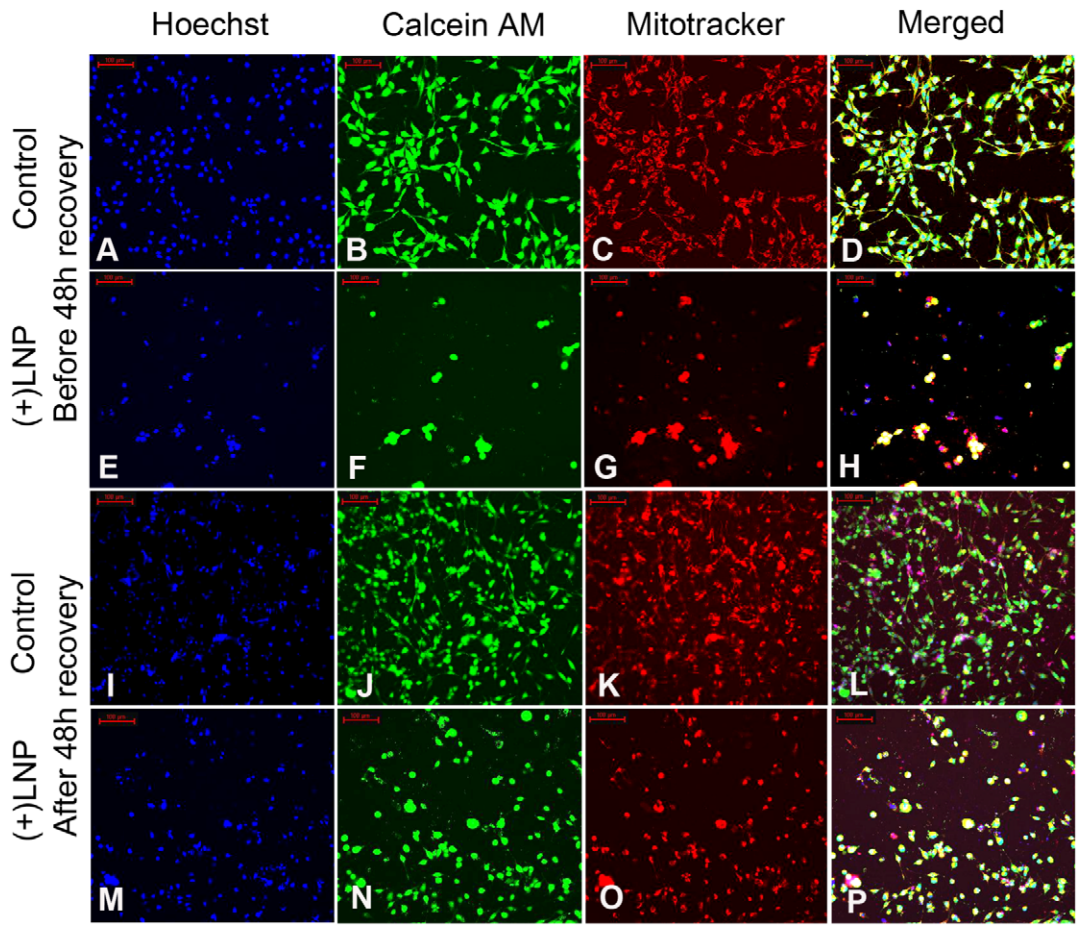


**Figure 2.** Representative images of fibroblasts treated with (+)LNPs or without (control) and their recovery 48 h post-culture. Images were taken using an In Cell Analyzer 2000 (GE Healthcare). Panels (A)–(D), untreated cells, 8 h, before recovery period; panels (E)–(H), (+) LNP cells treated for 8 h, before recovery; panels (I)–(L), untreated cells, 8 h, followed by a further 48 h of recovery time; and (M)–(P), (+) LNPs for 8 h followed by 48 h recovery in (+)LNP-free medium. (A), (E), (I), (M) Hoechst 33342 staining; (B), (F), (J), (N) calcein AM staining; (C), (G), (K), (O) Mitotracker staining; (D), (H), (L), (P) are merged images. Size bars: 100 $\mu$m.

the few calcein AM stained cells compared to the number of stained nuclei). This observation is in accord with the XTT results shown in figure 1(B) on the decrease in cell viability of cells treated with (100 $\mu$g ml$^{-1}$) (+)LNPs for 8 h. In contrast to this result, an increase in the cell density was observed after a further 48 h of culture, both for control (figures 2(I)–(L)) and for cells previously treated with (+) LNPs (figures 2(M)–(P)). This indicates the possibility that the treated cells may recover from the (+)LNP effect, showing an increase in the cell density and survival (as indicated by similar amount of calcein AM and Hoechst staining, observed after recovery, between treated and control cells).

In order to confirm that fibroblasts can indeed recover from toxic insult and to test the power of the high content analysis technology, we performed quantitative analysis of the experiments described above using In Cell 2000 software (GE Healthcare). Figure 3 shows a profile chart of multiple parameters (see details in table 2) obtained simultaneously by HCA of fibroblast cultures with (blue line) or without (red line) (+)LNPs for 8 h (upper chart) and for a further 48 h recovery after removal of this treatment (lower chart). Each line in the chart represents the mean value of the measurements for each parameter in the cell population. Analyses were performed from images taken by In Cell 2000 from at least four different fields in three different wells per condition. In this graphical way it is possible to observe the reproducibility of a given pattern for each analyzed condition that may be or may not be similar to another one. Using this robust methodology we wanted to understand whether treated cells differ from control cells and whether the population of treated cells is able to become more similar in its pattern to the control cells following a recovery period of 48 h. Representative parameters that were selected for analysis according to the labels used in the assays, which stained the cytoplasm, mitochondria and nuclear cell compartments are summarized in table 2 and plotted in figure 3.

Figure 3 indicates that several parameters differ between the two time points in culture while others are less distinct. Altogether, the profile chart of several cellular parameters determined by the HCA software strongly indicates that the 48 h of additional culture after (+)LNP removal allows the fibroblasts to recover from the cytotoxic effect induced by the exposure to (+)LNPs for 8 h. This is reflected, at first sight, by the increase in cell count observed in the profile chart for cells

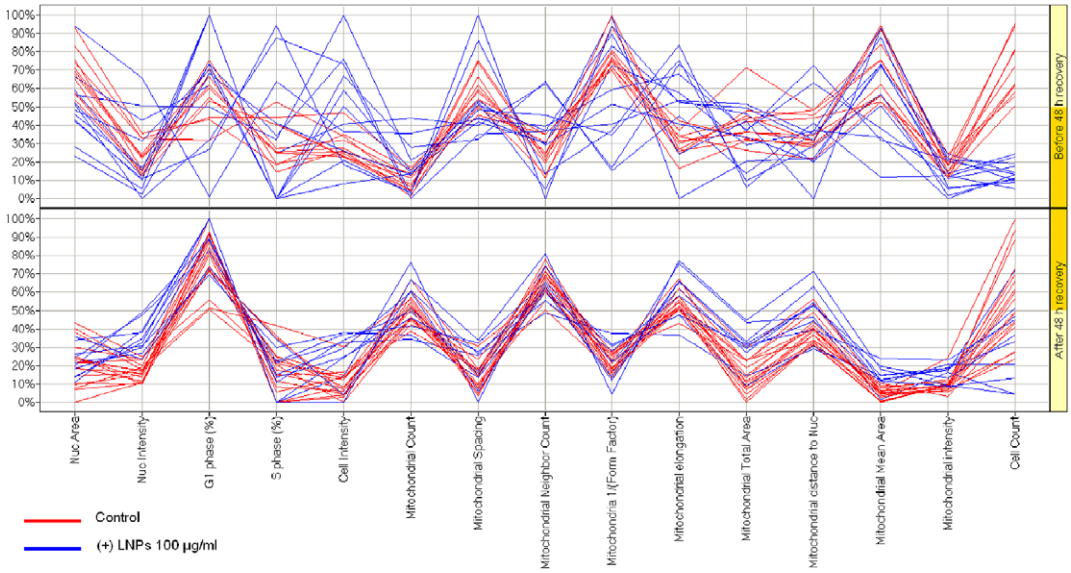


**Figure 3.** Profile charts of selected image-based measures of human primary fibroblasts cultured with or without cationic nanoparticles obtained from HCA. 100 $\mu$g ml$^{-1}$(+)LNPs (blue lines) or mock treated (red lines, control) fibroblasts cultured for 8 h, either immediately after (+)LNP removal (upper graph) or after a further 48 h culture in (+)LNP-free medium, allowing recovery (lower chart) of the cells from the cytotoxic insult. The cells were stained for 30 min at 37 °C with Hoechst 33342, calcein AM and Mitotracker. Images were acquired with the In Cell Analyzer 2000 (GE Healthcare) and analyzed using the In Cell Investigator 1.6 software. Each line represents a given field of a given triplicate. The parameters shown in the chart are detailed in table 2.

**Table 2.** Description of selected parameters analyzed in the imaged cells using HCA software.

| Parameter tested | Description |
|---|---|
| Nuclear area | Area of identified nucleus according to Hoechst staining |
| Nuclear intensity | Mean nuclear intensity in the cell according to Hoechst staining |
| G1 phase (%) | Percentage of cells in the population that according to the previous calibration of the nuclear area in the population were classified as being in the G0/G1 phase of the cell cycle |
| S phase (%) | Percentage of cells in the population that according to the previous calibration of the nuclear area in the population were classified as being in the S phase of the cell cycle |
| Cell intensity | Average intensity of pixels within the cytoplasm region (within the calcein AM channel). Since the cellular stain used is an indicator of viability, this parameter is directly related to viability. A weak signal is indicative of cell death |
| Mitochondrial count | Number of inclusions stained by Mitotracker attributed to the cell. Reflects mitochondrial activity and mitochondrial aggregation, which is related to cytotoxic effects |
| Mitochondrial spacing | Measures the inter-inclusion distance, determined by the sphere of influence adjacency rule (averaged by all Mitotracker stained inclusions within the cell) |
| Mitochondrial neighbor count | Number of neighboring mitochondrial inclusions, determined by the sphere of influence adjacency rule (averaged by all inclusions within the cell) |
| Mitochondrial 1/(formfactor) | Mean inclusion roundness index (averaged by all inclusions within the cell). Value ranges from 1 to infinity, where 1 is a perfect circle. Mitochondrial $1/(\text{form factor}) = \text{perimeter}^2/(4\pi \times \text{area})$ |
| Mitochondrial elongation | Mean ratio of the short axis of the inclusion to the long axis of the inclusion (averaged by all inclusions within the cell). If the value is 1 then the object is center-symmetric (not elongated) |
| Mitochondrial total area | Total area of mitochondrial inclusions attributed to the cell. Gives an indication of mitochondrial activity |
| Mitochondrial distance to nucleus | Mean distance from the center of gravity of the mitochondrial inclusion to the center of gravity of the nucleus (averaged by all inclusions within the cell). Gives an indication of mitochondrial aggregation, cell shrinkage due to changes in cell proliferation that could be a consequence of a recovery of the culture |
| Mitochondrial mean area | Mean area of mitochondrial inclusions (averaged by all inclusions within the cell). Gives an indication of mitochondrial activity and aggregation and could be clearly affected by a cytotoxic response |
| Mitochondrial intensity | Average intensity of pixels within mitochondrial inclusions. Gives an indication of mitochondrial activity |
| Cell count | Number of cells in the analyzed field. The most direct indication of culture toxicity/recovery |

that were previously exposed to (+)LNPs and then cultured for an additional 48 h upon removal of the cationic particles. Remarkably, this analysis allows us to determine the biological status of the cell population before and after treatment in a robust manner. For example, untreated cells and 8 h (+)LNP treated cells show a very different chart profile from that of the cell population after 48 h of recovery that is similar to its respective untreated control.

On merging figures 2 and 3, it becomes clear that fibroblasts possess the ability to recover from cytotoxic damage generated by exposure to (+)LNPs. This observation was also documented recently with gold nanoparticles, demonstrating the ability of dermal fibroblasts to recover after exposure to the gold nanoparticles for different times [18]. Moreover, looking at the profile charts in figure 3 we can see that since the main parameters that show changes between the charts (before and after recovery) are mostly related to mitochondria, it is more likely that the fibroblasts are affected by the (+)LNPs at the mitochondrial level. Thus, this technology allows us not only to determine that a given treatment causes toxicity or that following a certain time the cells are able to recover from such treatment, but also the mechanism of the observed toxicity. The mitochondrial mechanism of toxicity suggested by the HCA approach coincides with previously reported works showing the toxic effects of cationic LNPs on the mitochondria in primary leukocytes, epithelial cells, lymphoid, endothelial and hepatic cell lines [8, 13–17]. This strengthens HCA as a powerful methodology that also allows insights into the mechanism in the sub-cellular compartments, when different nanomaterials and treatments are being investigated at the cell population level.

### *3.4. Future perspectives*

In this study, we demonstrated the value of image-based high content analysis (HCA) to study different features of the cell simultaneously and detect changes in a designated cell population. The overall conclusion of our work is that image-based HCA allows measurement of numerous parameters simultaneously, thus allowing the construction of profile charts that are representative of cell populations under different culture conditions. In the case presented here, it enabled the identification of certain HCA parameters that reflected the biological recovery of the cells upon treatment with (+)LNPs. Our results suggest that mitochondrial toxicity is produced by the (+)LNPs. The simultaneous determination of different sub-cellular measures and their visualization as profile charts, showing either similarities or differences in the observed pattern, compared to a control of untreated cells, confer to HCA the potential to become a viable tool for high throughput screening (HTS) of new safe materials for drug delivery and tissue engineering.

## Acknowledgments

The authors wish to thank the Friends of Tel Aviv University in Mexico for their generous contribution to the establishment of an HCA cell screening facility for personalized medicine at Tel Aviv University. DP acknowledges the Levy family trust, the Marie Curie FP7 of the EU, Israel Science Foundation (award no 181/10) and I-core excellence center and the Alon Foundation for their financial support. This work is dedicated to the memory of Salomon and Moises Blanga Cohen.

## References

[1] Torchilin V P 2005 Recent advances with liposomes as pharmaceutical carriers *Nature Rev. Drug Discov.* **4** 145–60
[2] Peer D, Karp J M, Hong S, Farokhzad O C, Margalit R and Langer R 2007 Nanocarriers as an emerging platform for cancer therapy *Nature Nanotechnol.* **2** 751–60
[3] Peer D and Lieberman J 2011 Special delivery: targeted therapy with small RNAs *Gene Ther.*
[4] Peer D, Park E J, Morishita Y, Carman C V and Shimaoka M 2008 Systemic leukocyte-directed siRNA delivery revealing cyclin D1 as an anti-inflammatory target *Science* **319** 627–30
[5] Moghimi S M, Hunter A C and Murray J C 2001 Long-circulating and target-specific nanoparticles: theory to practice *Pharmacol. Rev.* **53** 283–318
[6] Akinc A *et al* 2009 Development of lipidoid-siRNA formulations for systemic delivery to the liver *Mol. Ther.* **17** 872–9
[7] Semple S C *et al* 2010 Rational design of cationic lipids for siRNA delivery *Nature Biotechnol.* **28** 172–6
[8] Kedmi R, Ben-Arie N and Peer D 2010 The systemic toxicity of positively charged lipid nanoparticles and the role of Toll-like receptor 4 in immune activation *Biomaterials* **31** 6867–75
[9] Zock J M 2009 Applications of high content screening in life science research *Comb. Chem. High Throughput Screen* **12** 870–76
[10] Ramirez C N *et al* 2011 Validation of a high-content screening assay using whole-well imaging of transformed phenotypes *Assay Drug Dev. Technol.* **9** 247–61
[11] Peer D and Margalit R 2004 Tumor-targeted hyaluronan nanoliposomes increase the antitumor activity of liposomal Doxorubicin in syngeneic and human xenograft mouse tumor models *Neoplasia* **6** 343–53
[12] Bachar G *et al* 2011 Hyaluronan-grafted particle clusters loaded with Mitomycin C as selective nanovectors for primary head and neck cancers *Biomaterials* **32** 4840–8
[13] Campbell R B *et al* 2002 Cationic charge determines the distribution of liposomes between the vascular and extravascular compartments of tumors *Cancer Res.* **62** 6831–6
[14] Dass C R 2004 Lipoplex-mediated delivery of nucleic acids: factors affecting in vivo transfection *J. Mol. Med.* **82** 579–91
[15] Lv H, Zhang S, Wang B, Cui S and Yan J 2006 Toxicity of cationic lipids and cationic polymers in gene delivery *J. Control. Release* **114** 100–9
[16] Hunter A C and Moghimi S M 2010 Cationic carriers of genetic material and cell death: a mitochondrial tale *Biochim. Biophys. Acta* **1797** 1203–9
[17] Moghimi S M, Symonds P, Murray J C, Hunter A C, Debska G and Szewczyk A 2005 A two-stage poly(ethylenimine)-mediated cytotoxicity: implications for gene transfer/therapy *Mol. Ther.* **11** 990–5
[18] Mironava T, Hadjiargyrou M, Simon M, Jurukovski V and Rafailovich M H 2010 Gold nanoparticles cellular toxicity and recovery: effect of size, concentration and exposure time *Nanotoxicology* **4** 120–37